


Review

Quantum Image Compression: Fundamentals, Algorithms, and Advances

Sowmik Kanti Deb and W. David Pan * 

Department of Electrical and Computer Engineering, University of Alabama in Huntsville, Huntsville, AL 35899, USA; sd0129@uah.edu

* Correspondence: pand@uah.edu

Abstract: Quantum computing has emerged as a transformative paradigm, with revolutionary potential in numerous fields, including quantum image processing and compression. Applications that depend on large scale image data could benefit greatly from parallelism and quantum entanglement, which would allow images to be encoded and decoded with unprecedented efficiency and data reduction capability. This paper provides a comprehensive overview of the rapidly evolving field of quantum image compression, including its foundational principles, methods, challenges, and potential uses. The paper will also feature a thorough exploration of the fundamental concepts of quantum qubits as image pixels, quantum gates as image transformation tools, quantum image representation, as well as basic quantum compression operations. Our survey shows that work is still sparse on the practical implementation of quantum image compression algorithms on physical quantum computers. Thus, further research is needed in order to attain the full advantage and potential of quantum image compression algorithms on large-scale fault-tolerant quantum computers.

Keywords: quantum computing; quantum image compression; quantum image processing



Citation: Deb, S.K.; Pan, W.D. Quantum Image Compression: Fundamentals, Algorithms, and Advances. *Computers* **2024**, *13*, 185. <https://doi.org/10.3390/computers13080185>

Academic Editors: Selene Tomassini, M. Ali Akber Dewan and Paolo Bellavista

Received: 17 May 2024
Revised: 13 July 2024
Accepted: 22 July 2024
Published: 25 July 2024



Copyright: © 2024 by the authors. Licensee MDPI, Basel, Switzerland. This article is an open access article distributed under the terms and conditions of the Creative Commons Attribution (CC BY) license (<https://creativecommons.org/licenses/by/4.0/>).

1. Introduction

In recent years, in accordance with Moore's law [1], the computing ability of electronic computers has exponentially increased. However, the growth in power of CPUs has plateaued in over the last few years due to various constraints, prompting the search for alternative methods to boost computational performance. In 1982, Richard Feynman, an American theoretical physicist, introduced the concept of quantum computing. This innovative model leverages quantum mechanics principles like superposition and entanglement to enhance data storage, processing, and transmission capabilities far beyond those of traditional computers [2]. The potential of quantum computing was further underscored by Peter Shor's introduction of a quantum algorithm for prime number factorization in 1994 [3], and by Lov Grover's quantum search algorithm in 1996 [4].

As the field of digital image processing evolves, it faces the challenge of handling an ever-growing volume and complexity of images, propelled by advances in pattern recognition, image understanding, and the development of sophisticated image sensors. Traditional image processing algorithms, foundational to numerous applications within information science, are inherently parallel in nature, demanding extensive computational resources for execution. The surge in image quantity and resolution has rendered these classical algorithms increasingly time-consuming and hardware-intensive. In response to these challenges, the integration of quantum computing into image processing emerges as a promising solution. Quantum computing utilizes qubits for data storage and leverages the properties of quantum physics, such as superposition and entanglement, to offer unparalleled parallel processing capabilities. This shift in paradigm provides a significant improvement in efficiency for tasks related to image processing.

The quantum approach to image processing significantly reduces the computational complexity associated with storing and manipulating large sets of image data. While a

classical computer requires exponential resources $O(n \times 2^n)$ to store sequences of n -bit length, a quantum computer can achieve this with linear complexity $O(n)$ [5]. Moreover, operations that are inherently sequential and resource-intensive on classical computers, such as bitwise inversion, can be executed more efficiently on quantum computers. This is due to the quantum computer's ability to perform operations on entangled qubits in parallel, dramatically reducing the time and resources needed for complex image processing tasks. This innovative method of leveraging quantum computing for image processing not only accelerates classical algorithms but also paves the way for the development of novel quantum image processing algorithms. These improvements have the potential to completely transform the field by greatly decreasing time it requires to analyze data and the amount of hardware needed. This will allow for the development of more advanced image processing applications that need a lot of resources. Hence, how can we use the quantum computing technique for image processing is crucial for surpassing the constraints of conventional computational techniques. This advancement presents a novel opportunity to efficiently and effectively process digital images.

To process images in quantum state, we need to follow three steps as Figure 1, (i) prepare the image and store it into quantum state, (ii) process quantum image, (iii) processed digital image from quantum state. The quantum image compression and encryption techniques lie in the preparation of the image into quantum state. Similar to the traditional digital image compression, the quantum image compression methods have lossy and lossless compression.

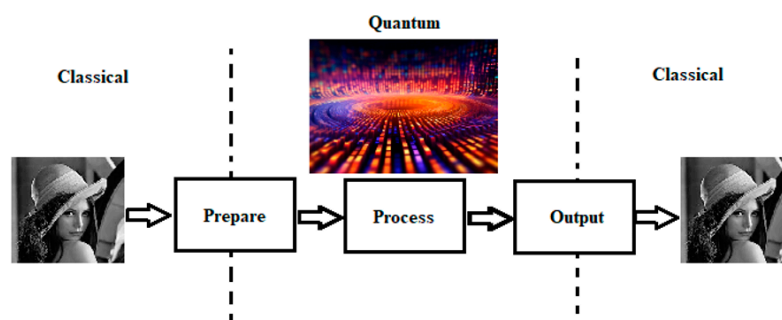


Figure 1. The processing steps of quantum image processing, converting the image from classical state to quantum state, then processing in quantum state, next convert the processed image from quantum to classical state as output.

The early 21st century witnessed several pivotal advancements aimed at enhancing the efficiency and quality of image compression techniques. In 2002, Lewis et al. introduced a method that utilized a two-dimensional orthogonal wavelet transform for compressing digital images. This innovative approach enabled the decomposition of images into coefficients that are localized both spatially and spectrally, offering a nuanced balance between preserving image quality and achieving substantial compression [6]. Another noteworthy development came in the form of an advanced bit plane coding strategy specifically designed for quantizing discrete cosine transform (DCT) coefficients [7]. This technique was lauded for its ability to deliver superior decoding quality compared to the JPEG2000 standard [8], which was the benchmark at the time. Kouda et al. introduced a hierarchical quantum neural network-based image compression scheme, assessing the utility of large quantum neural networks in tackling complex image compression scenarios [9]. This approach underscored the potential of quantum computing to revolutionize traditional practices by offering novel solutions that could outperform conventional algorithms in both efficiency and effectiveness. A significant challenge in image compression has always been the time-consuming nature of traditional image coding methods. To address this issue, Yang R. introduced a cutting-edge algorithm that employed a quantum BP (backpropagation) network for image compression [10]. This method not only accelerated the encoding process but also enhanced the quality of the reconstructed images, showcasing the synergy

between quantum computing and neural network methodologies in improving computational processes. In 2016, Yuen et al. unveiled an algorithm that combined discrete cosine transform (DCT) with the Secure Hashing Algorithm (SHA-1) for both compressing and encrypting images [11]. This dual-purpose algorithm highlighted the growing need for secure and efficient image processing techniques in an increasingly digital and interconnected world. In the same year, based on hyper-chaotic system Zhou et al. proposed an image encryption-compression scheme [12]. The same authors also published image encryption and compression scheme based on Mellin transform and compressive sensing [13]. In 2018, an image compression-encryption algorithms by combining hyper-chaotic system with discrete fractional random transform was introduced by Gong et al. [14].

While the above work is on the traditional images, as the field of quantum computing is advancing rapidly many of these classical techniques have been expanded to encompass the quantum realm. In this paper, we will focus on the quantum image processing and will discuss about the recent advancements in the field of quantum image compression. We start in Section 2 with a brief introduction to quantum computing. Readers already familiar with these fundamental concepts can skip Section 2 and proceed directly to Section 3.

2. Brief Introduction to Quantum Computing

2.1. Vector

Quantum states are mathematically expressed as vectors in a complex vector space called Hilbert space. Hilbert space is a fundamental framework in quantum mechanics because it can effectively capture the probabilistic and superpositional characteristics of quantum systems. The nomenclature used to represent vectors in Hilbert space is a distinctive and sophisticated formalism, generally known as Dirac notation, or more informally, the “bra-ket” notation [15].

$$|\psi\rangle = \begin{bmatrix} a_1 \\ a_2 \\ \vdots \\ a_n \end{bmatrix}, \quad (1)$$

In Dirac notation, a vector (representing a quantum state) in Hilbert space is symbolized by a ket, denoted as $|\psi\rangle$, where $|\cdot\rangle$ signifies the ket and ψ is a label that identifies the specific quantum state. The ket is a column vector that encompasses all the essential information required to completely explain the quantum state within the mathematical framework of quantum mechanics. Complementary to the ket is the bra, denoted as $\langle\phi|$, where $\langle\cdot|$ represents the bra, and ϕ is a label for the vector. The bra is essentially the conjugate transpose of the ket. In more concrete terms, if the ket represents a column vector, then the bra represents a row vector, with its complex elements conjugated. The usage of this bra vector is essential in the construction of quantum mechanical algorithms, particularly in the computation of probabilities and expectation values, which are key aspects of quantum mechanics.

The implementation of bra-ket notation brought about a significant transformation in the mathematical handling of quantum mechanics, providing a potent and intuitive mechanism for managing the abstract concepts essential to the theory. It simplifies the depiction of quantum processes, such as measurements and transformations, and offers a standardized framework for discussing and evaluating quantum states. It also enables the succinct definition of quantum mechanical processes, such as unitary transformations and observables. In summary, the bra-ket notation encapsulates the abstract and counterintuitive nature of quantum mechanics in a mathematically rigorous yet accessible language, enabling the exploration and exploitation of quantum phenomena for computational purposes.

2.2. Tensor Products

The tensor product is a mathematical operation that combines vector spaces to create a bigger vector space.

1. Assume, we have a scalar α . $|v\rangle$ is an element in V space and $|w\rangle$ is an element in W space. Then we can write:

$$\alpha(|v\rangle \otimes |w\rangle) = (\alpha|v\rangle \otimes |w\rangle) = |v\rangle \otimes \alpha(|w\rangle), \quad (2)$$

2. Now if we have two elements, $|v_1\rangle, |v_2\rangle$ in V space and an element $|w\rangle$ in W space

$$(|v_1\rangle + |v_2\rangle) \otimes |w\rangle = |v_1\rangle \otimes |w\rangle + |v_2\rangle \otimes |w\rangle \quad (3)$$

3. Similarly, $|v\rangle$ in V space and $|w_1\rangle$ and $|w_2\rangle$ in W space

$$|v\rangle \otimes (|w_1\rangle + |w_2\rangle) = |v\rangle \otimes |w_1\rangle + |v\rangle \otimes |w_2\rangle \quad (4)$$

We can find the tensor product of two matrices X (dimension $m \times n$) and Y (dimension $i \times j$) as

$$X \otimes Y = \begin{bmatrix} x_{11}Y & x_{12}Y & \cdots & x_{1n}Y \\ x_{21}Y & x_{22}Y & \cdots & x_{2n}Y \\ \vdots & \vdots & \ddots & \vdots \\ x_{m1}Y & x_{m2}Y & \cdots & x_{mn}Y \end{bmatrix} \quad (5)$$

2.3. Quantum Bit

In a classical computer bit is the core component, which functions inside a binary system, alternating between two distinct states: 0 and 1. The binary system serves as the foundation for classical computing architectures, allowing for the representation, manipulation, and retention of data. Quantum computing, in contrast, presents a sophisticated and intricate alternative to the classical bit, known as the quantum bit or qubit. Qubits are fundamental units that encapsulate the laws of quantum physics, forming the essential foundation for both the theoretical and practical aspects of quantum computing. Qubits, unlike traditional bits, exist inside a mathematical domain that is more flexible and abstract, rather than being limited to the binary certainties of 0 and 1. This abstraction enables the conceptualization and advancement of quantum computing theory without being limited by the physical implementation in specific hardware platforms. Qubits, being very versatile mathematical entities, allow for extensive study of the potential of quantum computing, without being restricted by the limits of physical systems.

A qubit is characterized by its capacity to exist in states that extend beyond the binary values of 0 and 1. The ability to simultaneously exist in several states is demonstrated by the phenomenon called quantum superposition, in which a qubit occupies a state that is a combination of $|0\rangle$ and $|1\rangle$. Mathematically, the superposed state can be represented as:

$$|\psi\rangle = \alpha|0\rangle + \beta|1\rangle \quad (6)$$

where α and β denote the probability amplitudes. The amplitudes represent the probability of the qubit collapsing into either the $|0\rangle$ or $|1\rangle$ state when measured. A qubit's state is represented as a vector in a two-dimensional complex vector space, with $|0\rangle$ and $|1\rangle$ being the basis states used for computation. The basis states constitute an orthonormal basis set, serving as a structured framework for the definition and manipulation of qubits.

The superposition principle grants qubits the ability to exist in several states simultaneously, which is in striking contrast to the binary restriction of conventional bits. Quantum computers have the ability to process and interpret data in ways that are fundamentally distinct from traditional computing methods due to their multi-state nature. When a measurement is performed on a superposed qubit state $|\psi\rangle$, it collapses into one of its

component states, either $|0\rangle$ or $|1\rangle$. The probability of each event is defined by the square of the associated probability amplitude ($|\alpha|^2$ for $|0\rangle$ and $|\beta|^2$ for $|1\rangle$). The stochastic character of qubit measurement forms the basis for the quantum mechanical phenomena that quantum algorithms utilize for purposes such as encryption, search optimization, and simulation of quantum systems. Also,

$$|\alpha|^2 + |\beta|^2 = 1 \quad (7)$$

In quantum computing, $|0\rangle$ is expressed as:

$$|0\rangle = \begin{bmatrix} 1 \\ 0 \end{bmatrix} \quad (8)$$

In quantum computing, $|1\rangle$ is expressed as:

$$|1\rangle = \begin{bmatrix} 0 \\ 1 \end{bmatrix} \quad (9)$$

$$|\psi\rangle = \alpha|0\rangle + \beta|1\rangle = \begin{bmatrix} \alpha \\ \beta \end{bmatrix} \quad (10)$$

Let us consider a pair of qubits. From a classical perspective, a pair of bits has the capability to represent four unique values (00, 01, 10, 11) simultaneously. However, within a quantum system, two qubits have the ability to simultaneously exist in a superposition of all four of these states. Consequently, the two-qubit system can be characterized by a state vector that encompasses this superposition, denoting a quantum state that is a linear combination of its four fundamental states: $|00\rangle$, $|01\rangle$, $|10\rangle$, and $|11\rangle$. So, the quantum state for two qubit system can be written as:

$$|\psi\rangle = \alpha_{00}|00\rangle + \alpha_{01}|01\rangle + \alpha_{10}|10\rangle + \alpha_{11}|11\rangle \quad (11)$$

where

$$|\alpha_{00}|^2 + |\alpha_{01}|^2 + |\alpha_{10}|^2 + |\alpha_{11}|^2 = 1 \quad (12)$$

These four states can be represented as:

$$|00\rangle = |0\rangle \otimes |0\rangle = \begin{bmatrix} 1 \\ 0 \\ 0 \\ 0 \end{bmatrix} \quad (13)$$

$$|01\rangle = |0\rangle \otimes |1\rangle = \begin{bmatrix} 0 \\ 1 \\ 0 \\ 0 \end{bmatrix} \quad (14)$$

$$|10\rangle = |1\rangle \otimes |0\rangle = \begin{bmatrix} 0 \\ 0 \\ 1 \\ 0 \end{bmatrix} \quad (15)$$

$$|11\rangle = |1\rangle \otimes |1\rangle = \begin{bmatrix} 0 \\ 0 \\ 0 \\ 1 \end{bmatrix} \quad (16)$$

2.3.1. Qubit Measurements and Unit Circle Theory

The basic states of a qubit in quantum computing are represented by the states $|0\rangle$ and $|1\rangle$ in quantum physics. In a two-dimensional coordinate system, where the state $|0\rangle$ aligns with the X-axis and the state $|1\rangle$ aligns with the Y-axis, these states can be visually depicted. Every state has a basis vector: the vector for $|0\rangle$ is $[1\ 0]^T$, indicating that it is a unit vector along the X-axis; the vector for $|1\rangle$ is $[0\ 1]^T$, indicating that it is a unit vector along the Y-axis.

We can take into consideration additional vectors that create different angles with the X-axis in order to investigate the idea of superposition. For example, the vector $[1/\sqrt{2}\ 1/\sqrt{2}]^T$ can be used to represent a vector that forms a 45-degree angle with the X-axis. According to this vector, there is an equal chance that this qubit will be measured and found in the states of $|0\rangle$ or $|1\rangle$. This indicates that the quantum state is an equal superposition of $|0\rangle$ and $|1\rangle$. In addition, another vector that forms a 60-degree angle with the X-axis can be represented by the column vector $[1/2\ \sqrt{3}/2]^T$. This vector represents a quantum state that is not an equal superposition of $|0\rangle$ and $|1\rangle$. Instead, it has distinct probabilities for being observed in each state, with a greater likelihood for the state $|1\rangle$ due to the larger coefficient in the vector representation.

Thus, a qubit can be mathematically described as a unit vector within a two-dimensional complex vector space (Figure 2). When we apply this principle to the geometric model known as the “Bloch sphere”, the state $|0\rangle$ correlates to the X-axis, whereas the state $|1\rangle$ aligns with the Y-axis on this sphere. It is crucial to emphasize that any point on the surface of the Bloch sphere represents a qubit in a state of superposition, which is a weighted combination of the states $|0\rangle$ and $|1\rangle$. In the practice of quantum measurement, two primary approaches are utilized. The first is the measurement in the standard basis, also known as the computational basis, which corresponds precisely to the previously mentioned states $|0\rangle$ and $|1\rangle$. The second methodology incorporates measurements taken on an arbitrary basis, enabling the evaluation of the qubit’s state across various Bloch sphere orientations. The selection of these arbitrary bases is not obligatory and can be chosen to accommodate particular quantum computing tasks or algorithms, thereby offering a versatile structure for the assessment and application of quantum states.

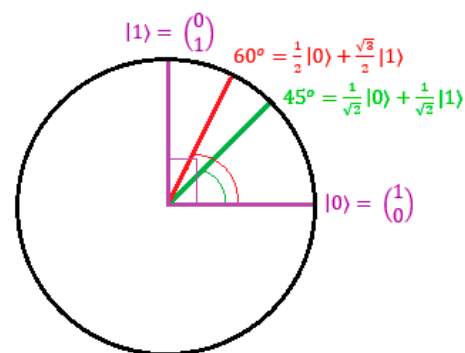


Figure 2. Unit circle representation on various angles. The vector $[1/\sqrt{2}\ 1/\sqrt{2}]^T$ can be used to represent a vector that forms a 45-degree angle with the X-axis and there is an equal chance that qubit will be measured and found in the states of $|0\rangle$ or $|1\rangle$. Another vector that forms a 60-degree angle with the X-axis can be represented by the column vector $[1/2\ \sqrt{3}/2]^T$. This vector represents a quantum state that is not an equal superposition of $|0\rangle$ and $|1\rangle$.

2.3.2. Measuring on Standard Basis

Let us assume, state $|S\rangle$ has an angle θ with $|0\rangle$ state in X axis. The figure is drawn in a 2D real space (Figure 3), and all of its amplitudes are real.

$$|S\rangle = a|0\rangle + b|1\rangle = \begin{pmatrix} \cos \theta \\ \sin \theta \end{pmatrix} \quad (17)$$

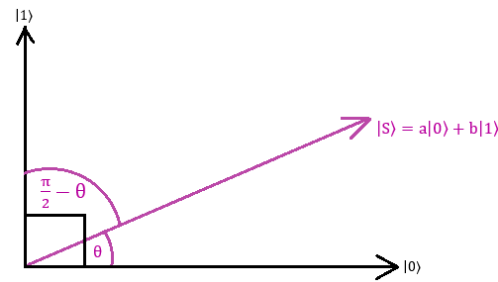


Figure 3. Projection on standard basis states. State $|S\rangle$ has an angle θ with $|0\rangle$ state in X-axis. Then the angle of $|S\rangle$ with $|1\rangle$ state would be $(\pi/2 - \theta)$.

From the figure, the state $|0\rangle$ has the probability $\cos^2 \theta$ and state $|1\rangle$ has the probability $\sin^2 \theta$, which can be written as $\cos^2 (\pi/2 - \theta)$. Thus, depending on the stated above probabilities, the state S is projected onto either the $|0\rangle$ state or $|1\rangle$ state.

2.3.3. Measuring on Arbitrary Basis

In this case, measurement is completed on any orthogonal basis rather than onto $|0\rangle$ and $|1\rangle$ basis. From Figure 4, state $|S\rangle$ is measure using $|u\rangle$ and $|u'\rangle$ basis. Here $|u\rangle$ has the probability $\cos^2 \theta$ and $|u'\rangle$ has the probability $\sin^2 \theta$. The amplitude of $|u\rangle$ and $|u'\rangle$ given by:

$$|u\rangle = \frac{1}{\sqrt{2}}|0\rangle + \frac{1}{\sqrt{2}}|1\rangle \quad (18)$$

$$|u'\rangle = -\frac{1}{\sqrt{2}}|0\rangle + \frac{1}{\sqrt{2}}|1\rangle \quad (19)$$

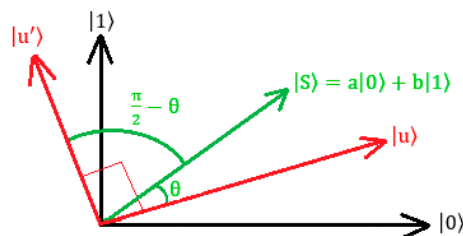


Figure 4. Projection onto arbitrary orthogonal basis states. State $|S\rangle$ is measured with respect to $|u\rangle$ and $|u'\rangle$. $|u\rangle$ and $|u'\rangle$ is measured with probability of $\cos^2 \theta$ and $\sin^2 \theta$, respectively.

These concepts will come in handy when we will talk about the FRQI (flexible representation of quantum images) representation of quantum images where rotation operation will be required.

2.4. Circuit and Gates

Logic gates are essential components in traditional digital circuits, responsible for manipulating and transforming information. They serve as the fundamental building blocks for complicated computing functions. Similarly, quantum circuits utilize a distinct set of logic gates that are specifically intended to function based on the principles of quantum mechanics. Quantum logic gates enable the manipulation of quantum information by applying unitary transformations to quantum states, allowing for the execution of logical operations. The mathematical description of these changes is commonly conveyed by matrices, which accurately capture the specific operation being applied to the quantum state.

One significant category of quantum logic gates is the single quantum gate (Figure 5). As the name implies, it only requires the participation of one qubit to perform its action. In contrast, multi-qubit gates are capable of performing quantum operations and interactions that are more intricate, as they involve two or more qubits. Quantum circuits employ

horizontal lines to represent qubits in their graphical depiction. The lines depicted in the schematic of a quantum circuit, commonly known as wires, represent the pathway through which quantum information travels. The symbol “U” is used to represent a single quantum gate on these wires. This symbol indicates the unitary operation that the gate performs on the qubit it interacts with. When $|\psi\rangle$ state is used as an input to this gate it gives $U|\psi\rangle$ as an output. Unitary transformations play a crucial role in the functioning of quantum gates. These transformations are invertible and maintain the norm of the quantum state, a necessity for quantum operations based on the principles of quantum physics. The utilization of a matrix representation for a quantum gate offers a potent means of comprehending and formulating quantum algorithms, as it enables the accurate computation of the gate’s impact on a certain quantum state.

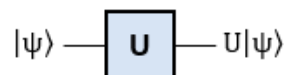


Figure 5. Single quantum gate.

The single quantum gate can be expressed in a matrix form:

$$|\psi\rangle = \begin{bmatrix} \alpha \\ \beta \end{bmatrix}, U = \begin{bmatrix} a & b \\ c & d \end{bmatrix} \quad (20)$$

$$U|\psi\rangle = \begin{bmatrix} a & b \\ c & d \end{bmatrix} \begin{bmatrix} \alpha \\ \beta \end{bmatrix} = \begin{bmatrix} a\alpha + b\beta \\ c\alpha + d\beta \end{bmatrix} \quad (21)$$

It is impossible to overstate the significance of single quantum gates in quantum computation. Although they are the most basic form of quantum gates, single quantum gate executes critical operations that are indispensable for quantum computation, including the initialization, manipulation, and preparation of measurements of qubits. The Pauli gates (X, Y, Z), which alter the state of a qubit in multiple dimensions, and the Hadamard gate, which generates superposition states, are both instances of single quantum gates. These gates function as the quantum equivalents of classical logic gates such as NOT and XOR, albeit within a domain where quantum states can be superimposed and entangled.

Hadamard gate:

$$H = \begin{bmatrix} \frac{1}{\sqrt{2}} & \frac{1}{\sqrt{2}} \\ \frac{1}{\sqrt{2}} & -\frac{1}{\sqrt{2}} \end{bmatrix} = \frac{1}{\sqrt{2}} \begin{bmatrix} 1 & 1 \\ 1 & -1 \end{bmatrix} \quad (22)$$

Applying the Hadamard gate to $|0\rangle$ state or $|1\rangle$ state:

$$H|0\rangle = \frac{1}{\sqrt{2}} \begin{bmatrix} 1 & 1 \\ 1 & -1 \end{bmatrix} \begin{bmatrix} 1 \\ 0 \end{bmatrix} = \frac{1}{\sqrt{2}}|0\rangle + \frac{1}{\sqrt{2}}|1\rangle = |+\rangle \quad (23)$$

$$H|1\rangle = \frac{1}{\sqrt{2}} \begin{bmatrix} 1 & 1 \\ 1 & -1 \end{bmatrix} \begin{bmatrix} 0 \\ 1 \end{bmatrix} = \frac{1}{\sqrt{2}}|0\rangle - \frac{1}{\sqrt{2}}|1\rangle = |-\rangle \quad (24)$$

So, by using the Hadamard H gate, the state $|0\rangle$ and $|1\rangle$ can be convert into a superposition state. The new state is known as $|+\rangle$ state and $|-\rangle$ state, respectively.

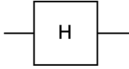
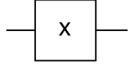
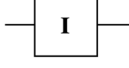
Pauli-X:

$$X = \begin{bmatrix} 0 & 1 \\ 1 & 0 \end{bmatrix} \quad (25)$$

The Pauli-X gate has the ability to change the state of a single qubit. That is why this gate is also called bit-flip or Not gate.

Table 1 shows some common single quantum gates.

Table 1. Example of some single quantum gates.

Gate Name/Operator	Circuit Diagram	Matrix Representation
Hadamard		$H = \frac{1}{\sqrt{2}} \begin{bmatrix} 1 & 1 \\ 1 & -1 \end{bmatrix}$
Pauli-X		$X = \begin{bmatrix} 0 & 1 \\ 1 & 0 \end{bmatrix}$
Identity		$I = \begin{bmatrix} 1 & 0 \\ 0 & 1 \end{bmatrix}$

Within the sophisticated realm of quantum computing, in addition to the simplicity and grace of individual quantum gates, there exists a more intricate category of quantum gates that require the participation of several qubits for their functioning. Multi-qubit quantum gates enhance the complexity and functionality of quantum circuits, allowing for a wider range of computational operations that exploit the distinct characteristics of quantum mechanics, such as entanglement and superposition, to perform tasks that are beyond the capabilities of single-qubit gates.

One prominent example of multi-qubit gates is the Controlled-NOT (CNOT) gate, which represents the idea of quantum control dynamics. The CNOT gate functions by manipulating two qubits, with one qubit acting as the control and the other as the target.

$$\text{CNOT} = \begin{bmatrix} 1 & 0 & 0 & 0 \\ 0 & 1 & 0 & 0 \\ 0 & 0 & 0 & 1 \\ 0 & 0 & 1 & 0 \end{bmatrix} \quad (26)$$

The CNOT gate operates by flipping the state of the target qubit, changing it from $|0\rangle$ to $|1\rangle$ or vice versa, only when the control qubit is in the state $|1\rangle$ as shown in the Equations (27)–(30). The conditional operation described here is the quantum equivalent of the conventional XOR gate. It showcases how quantum computing may imitate and expand upon traditional logic operations within a quantum context.

$$\text{CNOT}|00\rangle = \begin{bmatrix} 1 & 0 & 0 & 0 \\ 0 & 1 & 0 & 0 \\ 0 & 0 & 0 & 1 \\ 0 & 0 & 1 & 0 \end{bmatrix} \begin{bmatrix} 1 \\ 0 \\ 0 \\ 0 \end{bmatrix} = \begin{bmatrix} 1 \\ 0 \\ 0 \\ 0 \end{bmatrix} = |00\rangle \quad (27)$$

$$\text{CNOT}|01\rangle = \begin{bmatrix} 1 & 0 & 0 & 0 \\ 0 & 1 & 0 & 0 \\ 0 & 0 & 0 & 1 \\ 0 & 0 & 1 & 0 \end{bmatrix} \begin{bmatrix} 0 \\ 1 \\ 0 \\ 0 \end{bmatrix} = \begin{bmatrix} 0 \\ 1 \\ 0 \\ 0 \end{bmatrix} = |01\rangle \quad (28)$$

$$\text{CNOT}|10\rangle = \begin{bmatrix} 1 & 0 & 0 & 0 \\ 0 & 1 & 0 & 0 \\ 0 & 0 & 0 & 1 \\ 0 & 0 & 1 & 0 \end{bmatrix} \begin{bmatrix} 0 \\ 0 \\ 1 \\ 0 \end{bmatrix} = \begin{bmatrix} 0 \\ 0 \\ 0 \\ 1 \end{bmatrix} = |11\rangle \quad (29)$$

$$\text{CNOT}|11\rangle = \begin{bmatrix} 1 & 0 & 0 & 0 \\ 0 & 1 & 0 & 0 \\ 0 & 0 & 0 & 1 \\ 0 & 0 & 1 & 0 \end{bmatrix} \begin{bmatrix} 0 \\ 0 \\ 0 \\ 1 \end{bmatrix} = \begin{bmatrix} 0 \\ 0 \\ 1 \\ 0 \end{bmatrix} = |10\rangle \quad (30)$$

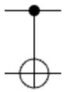
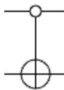

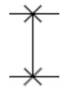
Expanding on the concept of conditional operations, the quantum computing also has the 0-Controlled-NOT (0CNOT) gate. This gate inverts the target qubit only when the control qubit is in the state $|0\rangle$. This gate expands the spectrum of quantum logic operations.

The Toffoli gate, also referred to as the CCNOT gate, is a significant expansion of the CNOT gate. It involves the use of two control qubits and one target qubit. The Toffoli gate performs a bit-flip operation on the target qubit exclusively when both control qubits are in the state $|1\rangle$. The significance of this gate in quantum computing lies in its ability to facilitate reversible computation, which is essential for the development of universal quantum computers. Also, as we explore farther into the domain of multi-qubit operations, the idea of scalability becomes apparent with the introduction of the n-CNOT gate. The gate expands the concept of conditional operation to n control qubits, providing a flexible method for coordinating intricate quantum processes that may be customized to meet the specific needs of advanced quantum algorithms.

Another important example of multi-qubit gate is the Swap gate. It facilitates the exchange of states between two qubits. The function of this gate is crucial in quantum algorithms as it allows for the reorganization of qubit states without impacting the overall quantum state of the system. This facilitates operations that necessitate particular qubit configurations.

Table 2 shows some common multiple quantum gates.

Table 2. Example of multiple quantum gates and their matrix representation.

Gate Name/Operator	Circuit Diagram	Matrix Representation
CNOT or CX		$\text{CNOT} = \begin{bmatrix} 1 & 0 & 0 & 0 \\ 0 & 1 & 0 & 0 \\ 0 & 0 & 0 & 1 \\ 0 & 0 & 1 & 0 \end{bmatrix}$
0CNOT		$0\text{CNOT} = \begin{bmatrix} 0 & 1 & 0 & 0 \\ 1 & 0 & 0 & 0 \\ 0 & 0 & 1 & 0 \\ 0 & 0 & 0 & 1 \end{bmatrix}$
Toffoli or CCX		$\text{Toffoli} = \begin{bmatrix} 1 & 0 & 0 & 0 & 0 & 0 & 0 & 0 \\ 0 & 1 & 0 & 0 & 0 & 0 & 0 & 0 \\ 0 & 0 & 1 & 0 & 0 & 0 & 0 & 0 \\ 0 & 0 & 0 & 1 & 0 & 0 & 0 & 0 \\ 0 & 0 & 0 & 0 & 1 & 0 & 0 & 0 \\ 0 & 0 & 0 & 0 & 0 & 1 & 0 & 0 \\ 0 & 0 & 0 & 0 & 0 & 0 & 0 & 1 \\ 0 & 0 & 0 & 0 & 0 & 0 & 1 & 0 \end{bmatrix}$
Swap		$\text{swap} = \begin{bmatrix} 1 & 0 & 0 & 0 \\ 0 & 0 & 1 & 0 \\ 0 & 1 & 0 & 0 \\ 0 & 0 & 0 & 1 \end{bmatrix}$

Having a basic understanding of these gates and how these work is very important because these gates are useful to build a quantum circuit. For instance, if we are working with the FRQI representation of quantum images, we need to understand the use of the Hadamard gate, Identity gate, Pauli-X gate, CNOT gate [16], etc. Another popular quantum image representation technique is NEQR (short for Novel Enhanced Quantum Representation) in which an image can be defined as:

$$|I\rangle = \frac{1}{2^n} \sum_{y=0}^{2^n-1} \sum_{x=0}^{2^n-1} \prod_{i=0}^{q-1} |c_{yx}^i\rangle |yx\rangle \quad (31)$$

To implement this, we need to use Hadamard gate, Toffoli gate, Swap gate [17], etc. We discuss this technique in detail in the next section. So, before jumping into the image processing part, knowing the basic concept of these gates are important because these will be required to represent the images in quantum state.

3. Quantum Image Representations

Before we delve into quantum image compression, we need to understand how an image can be represented in quantum state, since a number of quantum image representations have been proposed. The first attempt to represent an image in quantum system was proposed after introducing Qubit Lattice in 2003 [18]. Then in 2005 quantum superposition was introduced in Real Ket [19] to represent image. In 2010, Venegas et al. proposed entangled image which used quantum entanglement [20]. Le et al. also published their work FRQI or flexible representation of quantum images [16] in the same year. Here, they utilized an n-qubit sequence to represent the coordinate information. To store the color information of the image they used angle. An image in FRQI model can be represented as follows [16]:

$$|I(\theta)\rangle = \frac{1}{2^n} \sum_{i=0}^{2^{2n}-1} (\cos\theta_i|0\rangle + \sin\theta_i|1\rangle) \otimes |i\rangle \quad (32)$$

$$\theta_i \in \left[0, \frac{\pi}{2}\right], i = 0, 1, \dots, 2^{2n} - 1 \quad (33)$$

Here, $|i\rangle$ ($i=0, 1, \dots, 2^{2n} - 1$) are 2^{2n} computational basis quantum states and $\theta = (\theta_0, \theta_1, \dots, \theta_{2^{2n}-1})$ is the vector of angles encoding colors. Here the coordinate information is represented with $|i\rangle$ and the grey scale information is represented using $\cos\theta_i |0\rangle + \sin\theta_i |1\rangle$. This model can represent the greyscale information as well as the coordinate system of an image in quantum state properly.

This FRQI model was extended further in the following year and a new model called Multi-Channel Representation for Quantum Image (MCRQI) [21] was proposed, which also consider the RGB space. This model represents images as follows:

$$|I(\theta)\rangle = \frac{1}{2^{n+1}} \sum_{i=0}^{2^{2n}-1} |c_{RGB\alpha}^i\rangle \otimes |i\rangle \quad (34)$$

$$\begin{aligned} |c_{RGB\alpha}^i\rangle = & \cos\theta_{Ri}|000\rangle + \cos\theta_{Gi}|001\rangle + \cos\theta_{Bi}|010\rangle + \cos\theta_{\alpha i}|011\rangle \\ & + \sin\theta_{Ri}|100\rangle + \sin\theta_{Gi}|101\rangle + \sin\theta_{Bi}|110\rangle + \sin\theta_{\alpha i}|111\rangle \end{aligned} \quad (35)$$

As we can see, in MCRQI to store RGB channels and opacity, three qubits are required. Here, $\theta_{Ri}, \theta_{Gi}, \theta_{Bi}$ vectors represent the RGB colors and $\theta_{\alpha i}$ represents the channels.

In FRQI scheme while encoding the image pixels, normalized superposition state is utilized, allowing simultaneous operations on all pixels, thereby addressing the need for real-time processing in image applications. A number of algorithms have been introduced based on this principle. However, FRQI's restriction to one qubit per pixel for grayscale information makes certain complex color operations challenging.

The NEQR model for digital images representation, was introduced in 2013 by Zhang et al. [17], uses entangled qubit sequences to encode an image's grayscale and spatial information in a quantum superposition. This method converts grayscale values into binary using q qubits, improving simplicity and accessibility. The binary-encoded grayscale data are stored in a q-qubit sequence, whereas the coordinates for a 2^n -by- 2^n pixel image are retained in a $2n$ -qubit sequence. To better illustrate the algorithm, let us consider a 2-by-2 image as shown in Figure 6. In order to apply NEQR to an image, first $q + 2n$ qubits needs to be initialized to the $|0\rangle$ state. This is followed by applying identity (I) gates and Hadamard (H) gates to this initial state. Subsequently, the grayscale values for all pixels are established using $2n$ -CNOT gates. So, in the figure, to store the coordinate information H-gate needs to be applied to two of the ten $|0\rangle$ qubits. Then, 2-CNOT gates need to be

used to store the grayscale information. The quantum circuit for the NEQR preparation is shown in Figure 7.

$(240)_{10}$	$(68)_{10}$
$(11110000)_2$	$(01000100)_2$
00	01
$(148)_{10}$	$(73)_{10}$
$(10010100)_2$	$(01001001)_2$
10	11

Figure 6. A 2-by-2 example image where $(240)_{10}$ and $(11110000)_2$ is the intensity of pixel in decimal and binary at position 00. Same goes for other three pixels.

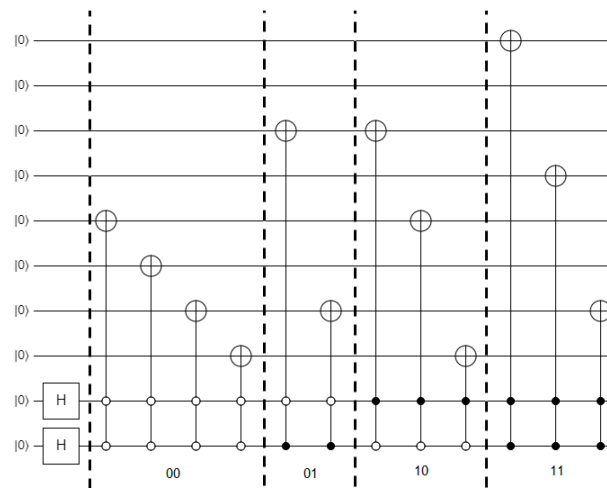


Figure 7. A 2-by-2 image represented in a quantum circuit by using the NEQR scheme.

The NEQR model is a substantial improvement over the FRQI model. NEQR requires more qubits than FRQI but solves the problem of reliably measuring grayscale information with a limited number of measurements. NEQR simplifies color operations, giving it a more practical and often useful framework in quantum image processing. However, both NEQR and FRQI have a constraint in that they are designed to store images that are strictly square because their horizontal and vertical coordinate lengths are equal. This limitation presents an issue for depicting images that are not square or rectangular, which are prevalent. To address this issue, the improved novel enhanced quantum representation (INEQR) [22] was introduced in 2015 by Jiang et al. INEQR allows for storing and processing rectangular images by supporting uneven horizontal and vertical coordinates. This improvement broadens the applicability of quantum image representations, making them more suitable for real-world scenarios where images may not have square dimensions.

GQIR or Generalized Quantum Image Representation was presented to represent non-square, rectangular images of arbitrary dimension by utilizing logarithmic coordinates [23]. Despite its versatility, GQIR adds redundancy to the representation process. The Novel Quantum Representation for Log-Polar Images (QUALPI) offers a framework for image representation in polar coordinates, diverging from conventional Cartesian-based methods [24]. In 2014, Li et al. introduced a new encoding approach for multi-dimensional color images called the n-qubit normal arbitrary superposition state (NASS). This method creatively encodes grayscale values using quantum states' angles and assigns certain states to represent different dimensions, enabling the compression of multi-dimensional color

images on a quantum computer [25]. In 2016, the FRQI method was improved, and a new model called the FRQCI or Flexible Representation for Quantum Color Image, which improved the management of color in quantum image representations [26]. Sang et al. developed the Novel Quantum Representation of Color Digital Images (NCQI) by integrating enhancements from MCRQI and NEQR within a similar period [27]. The new model modifies the qubits in NEQR from q to $3q$ to symbolize the RGB color channels, making color operations, such as intricate color transformations, much simpler to perform. Yet, a downside of the NCQI paradigm is the heightened need for qubits.

In 2018, Liu et al. introduced an Optimized Quantum Representation for Color Digital Images (OCQR) to tackle this problem [28]. OCQR requires fewer qubits, about one-third of what NCQI uses, to hold pixel values, while having a similar time complexity for preparing quantum pictures. OCQR optimizes computational resources by minimizing qubit usage and improves the efficiency of specific color changes. In 2017, the NEQR model was expanded to include Red–Green–Blue (RGB) color schemes by creating the Quantum Multi-Channel RGB Representation (QMCR) [29]. Although this new method demands more qubits than the MCRQI model, it streamlines the picture preparation process and allows for accurate image retrieval. In the same year, Jiang et al. introduced a new framework for three-dimensional imaging in the quantum realm, called the quantum point cloud [30]. This novel approach expands quantum image processing to 3D visual data, providing new opportunities for manipulating and analyzing digital images in quantum computing.

In the following year, BRQI (Bitplane Representation of Quantum Images) was published by Li et al. [31], which allows for altering color complements, reversing, and translating bitplanes within the BRQI framework. This BRQI method divides the grayscale values into eight different binary bits, converting a grayscale image into eight distinct bit planes. It requires three qubits to express the bitplane index, while n qubits are assigned to encode the spatial coordinates of the image. Moreover, Wang et al. in 2019, published a model where a bitplane is used to represent color digital images. They named this model QRCI [32]. An improved FRQI model called FRQCI was proposed by Li et al. [33]. Interestingly, in this model they talked about some image processing operators for pixel coordinate information and color representation. Khan explored FRQI and NEQR model further and came up with an improved flexible representation of quantum images (IFRQI) [34]. In this model, every pair of bits was represented using angle, enabling single qubit to store information equivalent to 2-bit grayscale values. This method significantly enhances the precision in retrieving the original image data. In the following year Grigoryan et al. published a new algorithm to store the images in quantum state by using Fourier transform representation [35]. In the same year, Wang et al. came up with a method called DQRCI (double quantum color images encryption scheme) in which two color images are stored into quantum superposition state simultaneously [36].

4. Quantum Image Compression

In this section, we provide a review of the literature in quantum image compression. To make it understandable for the readers this section is divided into two subsections. In the first subsection we talk about the papers focusing on direct methods and algorithms for compressing images using quantum computing techniques. These typically involve novel quantum algorithms that enhance or replace classical compression methods. In the second one, we give an overview of the papers that explore not only the quantum image compression technique but also quantum image representation, storage and retrieval.

4.1. Quantum Image Compression Techniques

In 2006, Yang et al. proposed a quantum vector quantization encoding algorithm for image compression [37]. This study presents a hybrid quantum-classical vector quantization (VQ) encoding algorithm that is more efficient than the pure quantum version. It requires fewer than \sqrt{N} (N = number of pixels) operations for most images and achieves close to a 100% success rate. The same group also published another work on image

compression by using the quantum discrete cosine transform (QDCT) [38]. The proposed algorithms for 1-D and 2-D DCT decrease the time complexity to $O(\sqrt{N})$ for 1-D and $O(N)$ for 2-D, in contrast to the classical complexities of $O(N \log_2 N)$ for 1-D and $O(N^2 \log_2 N)$ for 2-D. It also expands Grover's algorithm, known for its effectiveness in quantum searching, to tackle more complex unstructured search problems.

Nodehi et al. in 2009, proposed an image compression method for fractal images based on Functional Sized population Quantum Evolutionary Algorithm (FSQEA) [39]. The Quantum Evolutionary Algorithm (QEA) represents an emerging optimization technique that adopts probabilistic solution representation, proving to be especially effective for combinatorial challenges such as the Knapsack problem. Given that fractal image compression falls under the NP-Hard category, genetic algorithms (GAs) have traditionally been the go-to approach for such issues. However, the application of QEA to fractal image compression remains unexplored territory. In the paper, not only FSQEA for fractal image compression is proposed but also optimized by fine-tuning different parameters to enhance the performance, where it was shown that the PSNR of the proposed algorithm is better, i.e., 27.44 dB instead of 27.27 dB for GA. Notably, the time complexity of the FSQEA mirrors that of the original QEA, attributed to the fact that the average population size for the FSQEA is equivalent to that of the conventional QEA, and the number of function evaluations remains constant across both algorithms. Given the inherently time-intensive nature of fractal image compression, and the need for multiple iterations to ascertain optimal parameters, the study utilizes benchmark functions as a preliminary step. However, the temporal complexity of the FSQEA is similar to that of the original QEA because the average population size and the number of function evaluations are the same in both algorithms.

Qi et al. proposed an algorithm that uses Quantum Backpropagation (QBP) for image compression [40]. They showed a quantum neuron model that uses a combination of quantum gates, especially phase-shift and controlled-NOT gates as the basic building block for the operation. Incorporating the principles of traditional backpropagation (BP) they showed that the QBP network outperforms its classical BP counterpart. The work demonstrates a quicker learning rate ($\eta = 0.09$ compared to QNN with $\eta = 3.6$) as well as superior image compression capabilities (with a compression rate of $R = 0.16$ compared to QNN with 0.15).

Another work on fractal image compression (FIC) was presented by Du et al. in 2015 [41]. Grover's quantum search algorithm (QSA) was applied to accelerate the encoding process of FIC. Both theoretically and experimentally they showed that substantial amount of speedup was achieved by this method over the traditional FIC. Additionally, in terms of preserving the quality of retrieved images, the proposed QAFIC outperforms other contemporary FIC methods. A quantum image compression scheme based on JPEG was proposed by Jiang et al. in 2017 [42]. Figure 8 depicts the workflow of the JPEG based quantum image compression algorithm. As depicted in the workflow, first, the image is quantized, then the quantized JPEG coefficients are inputted into qubits and finally converted into pixel values. Compared with the Boolean expression compression (BEC) method, this scheme is less complicated and faster (with a running time of 0.164 s compared to 5.54 h in BEC), with high compression ratios (84.66% for the "cameraman" image compared to 69.07% in BEC).

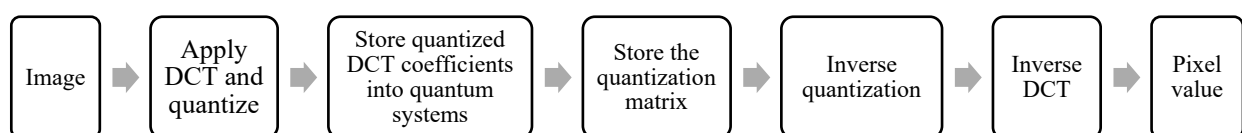


Figure 8. Workflow of JPEG based quantum image compression algorithm.

Pang et al. proposed a signal and image compression technique using the quantum discrete cosine transform (QDCT) [43]. In order to compress images and signals, this study introduces a quantum algorithm for the discrete cosine transform (DCT) that is specifically

engineered to be computationally more efficient than its classical counterpart. This is accomplished by the algorithm calculating the DCT coefficients concurrently and identifying the most significant coefficients. The conventional Grover's iteration is improved through the incorporation of a novel iteration method called the quantum DCT iteration (G_{DCT}), which is specifically designed for DCT operations and compression tasks.

The construction of the 1D-DCT using this method demonstrates an $O(\sqrt{N})$ complexity for a vector of size N . Conversely, the 2D-DCT computation for an N -by- N matrix manifests an $O(N)$ complexity. The quantum DCT algorithm was developed by taking advantage of two inherent properties of the DCT: its energy conservation capability and the fact that numerous DCT coefficients are insignificant and can therefore be excluded with minimal degradation to the quality of the reconstructed image. A study by Dai et al. introduces a quantum technique that utilizes the quantum DCT along with a 4-dimensional hyper chaotic Henon map to compress multiple images simultaneously [44]. Using QDCT, this method combines four grayscale images into a single quantum image, resulting in an efficient compression ratio that reduces the requirements for data transmission. Encryption involves using the 4D hyper-chaotic Henon map to manipulate the quantum image, uniformly spreading pixel values to create a large key space for increased security. A logistic map-guided quantum image cycle shift technique is used to scatter pixel data for improved encryption. The authors also showed by simulation that their model seems to be efficient with lower computational complexity ($O(n)$) than traditional picture encryption approaches ($O(n2^{3n})$ and $O(2^{6n})$).

In 2023, Ma et al. proposed a scheme to apply compression to quantum RGB images by using the quantum Haar wavelet transform (HQWT) and iterative quantum Fibonacci transform (IQFT) [45]. They converted multiple RGB images into a unified hybrid image. This hybrid image then undergoes compression at varying ratios using a measurement matrix built from Hadamard gates. The compressed image is then encrypted by using the Generalized Inverse Quantum Fourier Transform (IQFT), resulting in a compacted image form. The proposed scheme has total computation complexity of $O(n^3)$. In the following year, Wang et al. published a quantum version of autoencoder based on parameterized quantum circuits for image compression [46]. They combined quantum image processing with the machine learning, especially the autoencoder to apply image compression on the quantum images. Ji et al. proposed an image compression and reconstruction algorithm by leveraging the quantum network (QN) in 2024 [47]. QN is a network structure where the fundamentals of quantum mechanics are used to transmit and process information. In their approach, first the image is converted to a quantum state from classical state. Then this quantum state is used as an input for the quantum compression network. The measurements of the output state are converted into compressed image which are utilized to train the QN based on the gradient descent algorithm. Lastly, the simulation of compression of grayscale images is realized by this quantum algorithm. Haque et al. proposed a block-wise lossy SCMNEQR (state connection modification novel enhanced quantum representation) compression scheme for quantum gray-scale images [48]. Their algorithm was able to minimize the total computational time by 99.66% and 7.36% compared to JPEG and DCT-EFRQI (Direct Cosine Transform Efficient Flexible Representation of Quantum Image) approaches, respectively.

4.2. Quantum Image Storage, Representation, Compression, and Retrieval Techniques

In 2011, one of the pioneering works on quantum image processing was published by Le et al. [16]. A flexible representation of quantum images (FRQI) was proposed in this paper. Quantum image compression (QIC) aims to decrease the quantum resources necessary for preparing and reconstructing quantum images by lowering the number of simple quantum gates needed, which is crucial in both the theoretical and practical realms of quantum computing, as seen in the FRQI model, where simplifying basic gates such as controlled rotation gates is critical.

A way is suggested to combine these gates with identical rotation angles by leveraging the limited ability of the human visual system to differentiate between numerous colors, which enables a distinct range of color values for representation. Grouping controlled rotation operators with the same angles and combining their conditions can greatly decrease the required number of gates. We can consider an 8×8 pixel image as shown in Figure 9 with only two colors: blue and red. This image would need $64 C^6(\cdot)$ controlled-rotation gates for its initial quantum state preparation. Here the dot (\cdot) in these notations is a placeholder indicating that the gate can be applied to any arbitrary target gate. Categorizing these gates into two groups based on color can significantly decrease the total number. The 64 gates can be simplified to 4 as shown in Figure 10, resulting in a 93.75% reduction, by using simpler gates such as one $C^1(\cdot)$ and two $C^2(\cdot)$ gates for the red locations.

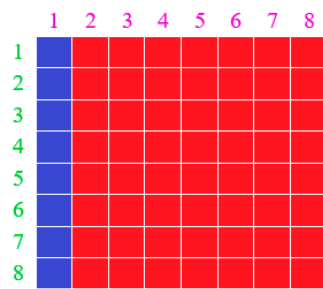


Figure 9. Two color 8×8 pixel image, 8 blue pixels and 56 red pixels.

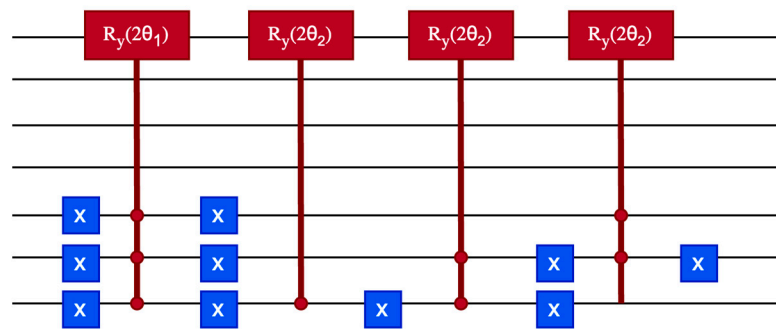


Figure 10. Minimized circuit for a two-color 8×8 pixel image. Here, X is the Pauli-X gates, θ is the vector of angles encoding colors (two in this case) and $R_y(2\theta_i)$ is the controlled-rotation gate.

The controlled-rotation gate is given by the following equation:

$$R_y(2\theta_i) = \begin{pmatrix} \cos \theta_i & -\sin \theta_i \\ \sin \theta_i & \cos \theta_i \end{pmatrix} \tag{36}$$

A key step in this process involves translating binary strings that represent pixel positions into Boolean minterms. Each binary digit is treated as a Boolean variable, with “1” represented by the variable (x) and “0” represented by its negation (\bar{x}). After organizing the gates by color, we can condense them by merging the binary strings of each color group into a unified Boolean expression. This phrase includes all the necessary conditions for the controlled-rotation gates of that group. An 8-position group in the blue color category as shown in Figure 11, which would have needed 8 individual gates, can be depicted by a single term in a simplified Boolean expression. This suggests that replacing the original eight gates with a single controlled-rotation gate can simplify the quantum circuit and decrease the quantum resources required for image representation.

The 8 position of blue pixels and their binary string and Boolean expression

0⟩	→	000000⟩	→	$\overline{x_5 x_4 x_3 x_2 x_1 x_0}$
8⟩	→	001000⟩	→	$\overline{x_5 x_4 x_3 x_2 x_1} x_0$
16⟩	→	010000⟩	→	$x_5 \overline{x_4 x_3 x_2 x_1} x_0$
24⟩	→	011000⟩	→	$x_5 x_4 \overline{x_3 x_2 x_1} x_0$
32⟩	→	100000⟩	→	$x_5 \overline{x_4 x_3 x_2} x_1 x_0$
40⟩	→	101000⟩	→	$x_5 x_4 \overline{x_3 x_2} x_1 x_0$
48⟩	→	110000⟩	→	$x_5 x_4 x_3 \overline{x_2} x_1 x_0$
56⟩	→	111000⟩	→	$x_5 x_4 x_3 x_2 \overline{x_1} x_0$

$$\begin{aligned} \text{Minimized Boolean expression} &= \overline{x_5 x_4 x_3 x_2 x_1 x_0} + \overline{x_5 x_4 x_3 x_2 x_1} x_0 + \overline{x_5 x_4 x_3 x_2} x_1 x_0 + \overline{x_5 x_4 x_3} x_2 x_1 x_0 + \\ & x_5 \overline{x_4 x_3 x_2 x_1} x_0 + x_5 \overline{x_4 x_3} x_2 x_1 x_0 + x_5 x_4 \overline{x_3 x_2} x_1 x_0 + x_5 x_4 x_3 \overline{x_2} x_1 x_0 \\ &= \overline{x_2 x_1 x_0} \end{aligned}$$

Figure 11. Boolean expression and its minimized expression for an 8-position group.

The QIC algorithm aims to decrease the number of controlled rotation gates within color groups by minimizing their Boolean expression, as depicted in Figure 12. The process begins with identifying places within the group of similar color and concludes with simplified Boolean expression.

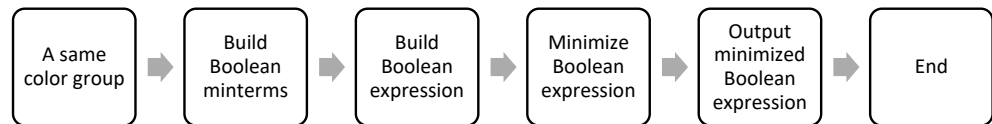


Figure 12. Quantum image compression flow chart.

In 2013, Li et al. proposed a method to store, retrieve and compress images in a quantum system [49]. More specifically, the authors proposed a compression algorithm where they achieve a lossless compression ratio of 2.058. In this algorithm, to compress an image, termed “newImage”, we first determine the number *m* of unique colors the image contains. Each color relates to a quantum state from the QSMC set, and these states are lined up in a quantum queue. The compression procedure involves scanning the “newImage” in a certain direction as shown in Figure 13, either row-wise starting from the second pixel of the first row (1,2) or column-wise starting from the second row’s first pixel (2,1). We record only the initial pixel of each continuous sequence of pixels with identical colors as we scan. When the scan encounters a pixel of a different color, it stops to record the color and sequence length before continuing from the last pixel of the uniform sequence. *s* is the length of the longest sequence of pixels with matching color. *n* is the number of pixels in the compressed “newImage”.

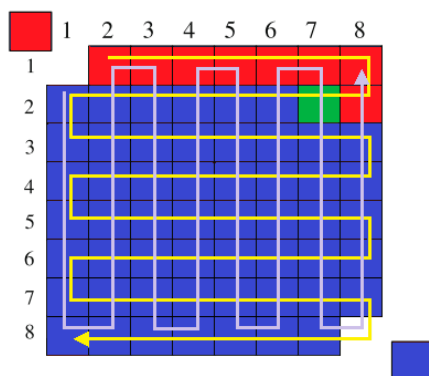


Figure 13. Scanning a 3-color 8 × 8 image by rows (indicated by the purple line) starting from the second pixel of the first row (1,2), and by columns (indicated by the yellow line) starting from the second row’s first pixel (2,1).

Next, a bijective function is created as:

$$E_4 : posNum \rightleftharpoons \gamma, \tag{37}$$

where $posNum = \{1, 2, \dots, m, m + 1, m + s\}$ and $\gamma = \{\gamma_1, \gamma_2, \dots, \gamma_{m+s}\} (\gamma_i = \frac{\pi(i-1)}{2(m+s-1)}, i \in \{1, 2, \dots, m + s\})$. $R_y(2\gamma_i)$, which is rotation operator given by Equation (38), converts state $|0\rangle$ to $m+s$ states.

$$R_y(2\gamma_i) = \begin{bmatrix} \cos \gamma_i & -\sin \gamma_i \\ \sin \gamma_i & \cos \gamma_i \end{bmatrix}, (i = 1, 2, \dots, m + s) \tag{38}$$

$$\begin{cases} |\bar{\omega}_i\rangle = \cos \gamma_i |0\rangle + \sin \gamma_i |1\rangle, i \in \{1, 2, \dots, m\} \\ |x_i\rangle = \cos \gamma_{m+i} |0\rangle + \sin \gamma_{m+i} |1\rangle, i \in \{1, 2, \dots, m\} \end{cases} \tag{39}$$

Here $|\bar{\omega}_j\rangle$ is the j th position of queue Q_1 and $|x_i\rangle$ represents an integer i . $|\bar{\psi}_i\rangle$ represents the i th pixel and can be defined as:

$$|\bar{\psi}_i\rangle = \begin{cases} |\bar{\omega}_j\rangle \otimes |u_x\rangle, i = 1, |u_x\rangle \in QSNC, x \in \{1, 2, \dots, N\} \\ |\bar{\omega}_j\rangle \otimes |u_y\rangle, i = n, |u_y\rangle \in QSNC, y \in \{1, 2, \dots, N\} \\ |\bar{\omega}_j\rangle \otimes |x_k\rangle, i \in \{2, 3, \dots, n - 1\}, k \geq 2 \\ |\bar{\omega}_j\rangle, i \in \{2, 3, \dots, n - 1\}, k = 1 \end{cases} \tag{40}$$

where u_x is the coordinate of the first pixel and u_y is the coordinate of the last pixel of the newImage, k represents consecutive pixels of same color depending on the direction of the scanning. After that $|\bar{\psi}_i\rangle$ is stored in another quantum queue Q_2 and the process is repeated. Suppose three colors in Figure 13 are represented, respectively, by $|v_r\rangle, |v_g\rangle, |v_b\rangle$ and saved in Q_1 . Q_2 has five states as follows: $|\bar{\psi}_1\rangle = |\bar{\omega}_1\rangle \otimes |u_1\rangle, |\bar{\psi}_2\rangle = |\bar{\omega}_1\rangle \otimes |x_8\rangle, |\bar{\psi}_3\rangle = |\bar{\omega}_2\rangle, |\bar{\psi}_4\rangle = |\bar{\omega}_3\rangle \otimes |x_{53}\rangle, |\bar{\psi}_5\rangle = |\bar{\omega}_3\rangle \otimes |u_{120}\rangle$. The compressed image stored in Q_1 and Q_2 is shown in Figure 14.

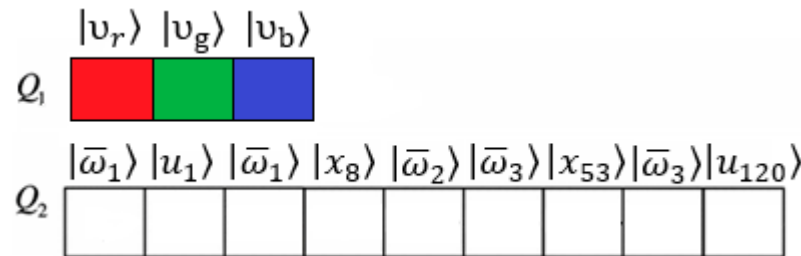


Figure 14. The compressed image stored in Q_1 and Q_2 .

Another milestone in quantum image processing was the NEQR model [17] proposed in 2013 by Zhang et al., in which 15X compression ratio on quantum images was achieved. While FRQI relies on one qubit per pixel to store grayscale data, which restricts compression to areas with consistent grayscale values, NEQR stores grayscale data by distributing it among a series of qubits, enabling optimization of each qubit separately. By employing Boolean expression minimization, NEQR can obtain higher compression ratios for quantum images by simplifying the preparation of each qubit individually. An operation set Φ consists of all the quantum operations of quantum image preparation can be expressed as

$$\phi = \bigcup_{Y=0}^{2^n-1} \bigcup_{X=0}^{2^n-1} \bigcup_{i=0}^{q-1} \phi_{YX}^i, \phi_{YX}^i \in \{I, 2n - \text{CNOT}\} \tag{41}$$

where ϕ_{YX}^i represents the quantum operation for the i th qubit. These operations can be categorized into q groups as shown in the following equation:

$$\phi = \bigcup_{Y=0}^{2^n-1} \bigcup_{X=0}^{2^n-1} \bigcup_{i=0}^{q-1} \phi_{YX}^i = \bigcup_{i=0}^{q-1} \left(\bigcup_{Y=0}^{2^n-1} \bigcup_{X=0}^{2^n-1} \phi_{YX}^i \right) = \bigcup_{i=0}^{q-1} \phi_i \quad (42)$$

Depending on the value of C_{YX}^i , the style of the operation ϕ_{YX}^i will change such that, when $C_{YX}^i = 0$, ϕ_{YX}^i will be the identity gate I . Otherwise, it will be $2n - CNOT$ qubit gate. This will invert the i th qubits in the color qubit sequence when the pixel position is (Y, X) . Thus ϕ can be written as:

$$\begin{aligned} \phi &= \bigcup_{Y=0}^{2^n-1} \bigcup_{X=0}^{2^n-1} \phi_{YX}^i \\ \phi &= \left(\bigcup_{Y=0}^{2^n-1} \bigcup_{X=0, C_{YX}^i=0}^{2^n-1} I \right) \cup \left(\bigcup_{Y=0}^{2^n-1} \bigcup_{X=0, C_{YX}^i=1}^{2^n-1} (2n - CNOT)_{YX} \right) \end{aligned} \quad (43)$$

The identity operation will not affect the quantum state; hence, the operation can be ignored from the first part in the i th group of quantum operation. The espresso algorithm [50] which is used in the second part of the operation, compresses the control information of controlled not gates. The espresso algorithm is a program use to reduce the complexity of digital logic gate circuits by using heuristic and specific algorithms.

$$\bigcup_{Y=0}^{2^n-1} \bigcup_{X=0, C_{YX}^i=1}^{2^n-1} YXEspresso \rightarrow \bigcup_{K_i} K_i \quad (44)$$

The expression builds a new quantum controlled-not gates $\bigcup_{K_i} K_i - CNOT$ for the new i th group ϕ'_i by providing the equivalent and compact control information sets $\bigcup_{K_i} K_i$. So, the new circuit will be given by,

$$\phi' = \bigcup_{i=0}^{q-1} \phi'_i = \bigcup_{i=0}^{q-1} \bigcup_{K_i} K_i - CNOT \quad (45)$$

Figure 15 shows the workflow for image compression in the NEQR algorithm.

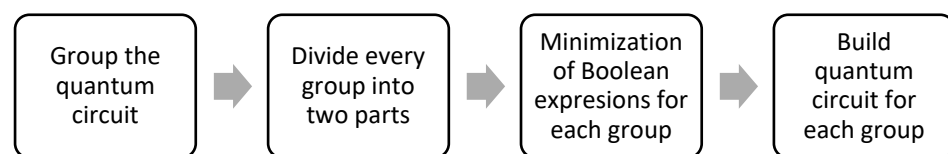


Figure 15. Workflow of image compression in the NEQR algorithm.

A study from 2014 shows the multidimensional color image compression based on quantum amplitudes and phases [25]. Both the lossless and lossy quantum image compression algorithms were developed. About 72.6 compression ratio was achieved by this algorithm. For lossless compression, the process is divided into two steps. The first step is dimensionality reduction and sorting algorithm for a k -dimensional color image (called DRS). In the second step, the lossless compression algorithm was applied for quantum images (LCQI). For lossy image compression Quantum Fourier Transform (QFT) was used to generate a NASS (n -qubit normal arbitrary superposition state) state $|\psi_A\rangle$. About 1.4 quantum compression ratio was achieved in this case. They also applied QWT (Quantum Wavelet Transform) instead of QFT and achieved 1.5 quantum compression ratio. In 2022, Amankwah et al. published a paper that introduced quantum compression for

N-dimensional images [51]. They applied their algorithm to prepare an FRQI state, which reduced the number of necessary gates by up to 90%, without lowering the image quality. Haque et al. published a paper on quantum image representation and compression technique using DCT-EFRQI (Direct Cosine Transform Efficient Flexible Representation of Quantum Image) in 2023 [52]. Both experimental and theoretical results showed that the proposed DCT-EFRQI had better compression ratio compared with EFRQI (Efficient Flexible Representation of Quantum Image). For example, for the “cameraman” image, the proposed algorithm had compression ratio of 8.4543:1 compared to 2.5864:1 for EFRQI. The work showed that DCT-EFRQI provided twice as much compression on medium-size images (512×512) than on large-size images (1024×1024).

5. Conclusions

Quantum image compression applies the laws of quantum mechanics to improve the effectiveness of image data reduction and compression. It utilizes qubits to encode image data by taking advantage of superposition and entanglement to process and compress images in a way that the classical algorithms cannot match. By leveraging quantum parallelism, these methods can theoretically achieve compression tasks at speeds unattainable by classical computers, with potentially higher compression ratios and lower losses of quality. Moreover, the inherent properties of quantum systems, like the ability to handle vast amounts of data simultaneously, make quantum image compression particularly suited for high-resolution and high-dimensional imaging applications, such as medical imaging, satellite imagery, and large-scale video data. However, the practical application of quantum image compression is still in its nascent stages. The field faces substantial challenges that stem primarily from the limitations of current quantum technology. These include the instability of quantum states (decoherence), the high error rates of quantum operations, the complexity of quantum circuit design, and the need for robust quantum error correction methods. We believe that rapid advances in quantum systems and hardware in the coming years will help address these constraints. Moreover, there are plenty of opportunities to conduct further research on quantum algorithms that mimic the classical transform coding methods like Fourier transforms or wavelet transforms, where we utilize the properties of quantum bits to perform quantum-specific transformations on quantum states representing images. This could lead to more efficient transformations, reducing the time and resources needed for encoding and decoding images. Moreover, if quantum entanglement can be utilized to compress correlated regions within an image by entangling qubits that represent similar or related image features (like colors or edges), it might be possible to reduce the overall number of qubits needed to represent an image, effectively compressing the image data. Furthermore, quantum machine learning models can be designed to learn optimal compression strategies based on the image content. These models could identify patterns and features in image data that classical algorithms might overlook and use these insights to compress images more effectively. Also, a hybrid algorithm can be developed where the initial stages of image processing and feature extraction are performed using classical techniques, and the heavy lifting of actual data compression is conducted on quantum hardware. This could make quantum image compression more practical and accessible with current technology. But it is needless to say, the development of scalable quantum computers that can handle real-world image compression tasks remains a significant hurdle. Work is still sparse on the practical feasibility in the implementation of quantum image compression algorithms on physical quantum computers, where a huge amount of quantum gates will present challenges on achieving fidelity by dealing with noise and decoherence [53]. According to IBM’s quantum road map “<https://www.ibm.com/roadmaps/quantum/2024/>” (accessed on 14 July 2024)”, in about ten years or so, quantum computers will be able to support 2000 qubits working in a distributed 100,000-qubit machine, with distributed software tools that enable noise-free quantum computations working seamlessly with classical computations. While there seems to be a long way to go before we can attain the full advantage and potential of the many algorithms we have discussed above, the

future of quantum image compression is bright as we are entering into the new age of quantum-centric computing.

Author Contributions: Conceptualization, W.D.P.; Methodology, S.K.D. and W.D.P.; Validation, S.K.D. and W.D.P.; Formal Analysis, S.K.D., W.D.P.; Investigation, S.K.D. and W.D.P.; Resources, S.K.D. and W.D.P.; Data Curation, S.K.D. and W.D.P.; Writing—Original Draft Preparation, S.K.D. and W.D.P.; Writing—Review & Editing, S.K.D. and W.D.P.; Visualization, S.K.D.; Supervision, W.D.P.; Project Administration, W.D.P. All authors have read and agreed to the published version of the manuscript.

Funding: This research received no external funding.

Conflicts of Interest: The authors declare no conflict of interest.

References

1. Moore, G. Cramming more components onto integrated circuits. *Proc. IEEE* **1998**, *86*, 82–85. [[CrossRef](#)]
2. Feynman, R.-P. Simulating physics with computers. *Int. J. Theor. Phys.* **1982**, *21*, 467–488. [[CrossRef](#)]
3. Shor, P.W. Algorithms for quantum computation: Discrete logarithms and factoring. In *Proceedings 35th Annual Symposium on Foundations of Computer Science*; IEEE: Piscataway, NJ, USA, 1994; pp. 124–134.
4. Grover, L.K. A fast quantum mechanical algorithm for database search. In *Proceedings of the 28th Annual ACM Symposium on the Theory of Computing*, ACM, Philadelphia, PA, USA, 22–24 May 1996; pp. 212–219.
5. Wang, Z.; Xu, M.; Zhang, Y. Review of Quantum Image Processing. *Arch. Comput. Methods Eng.* **2022**, *29*, 737–761. [[CrossRef](#)]
6. Lewis, A.S.; Knowles, G. Image compression using the 2-D wavelet transforms. *IEEE Trans. Image Process.* **2002**, *1*, 244–250. [[CrossRef](#)]
7. Ponomarenko, N.; Lukin, V.; Egiazarian, K.; Astola, J. DCT based high quality image compression. In *Proceedings of the Image Analysis, Scandinavian Conference, SCIA 2005*, Joensuu, Finland, 19–22 June 2005; Volume 3540, pp. 1177–1185.
8. Taubman, D.S.; Marcellin, M.W. JPEG2000: Standard for interactive imaging. *Proc. IEEE* **2002**, *90*, 1336–1357. [[CrossRef](#)]
9. Kouda, N.; Matsui, N.; Nishimura, H. Image compression by layered quantum neural networks. *Neural. Process. Lett.* **2002**, *16*, 67–80. [[CrossRef](#)]
10. Yang, R.; Zuo, Y.J.; Lei, W.J. Researching of image compression based on quantum BP network. *Telkomnika Indones. J. Elect. Eng.* **2013**, *11*, 6889–6896.
11. Yuen, C.H.; Wong, K.W. A chaos-based joint image compression and encryption scheme using DCT and SHA-1. *Appl. Soft Comput.* **2011**, *11*, 5092–5098. [[CrossRef](#)]
12. Zhou, N.R.; Pan, S.M.; Cheng, S. Image compression-encryption scheme based on hyper-chaotic system and 2D compressive sensing. *Opt. Laser Technol.* **2016**, *82*, 121–133. [[CrossRef](#)]
13. Zhou, N.R.; Li, H.L.; Wang, D.; Pan, S.M.; Zhou, Z.H. Image compression and encryption scheme based on 2D compressive sensing and fractional Mellin transform. *Opt. Commun.* **2015**, *343*, 10–21. [[CrossRef](#)]
14. Gong, L.; Deng, C.; Pan, S.; Zhou, N. Image compression-encryption algorithms by combining hyper-chaotic system with discrete fractional random transform. *Opt. Laser Technol.* **2018**, *103*, 48–58. [[CrossRef](#)]
15. Dirac, P.A.M. A new notation for quantum mechanics. *Math. Proc. Camb. Philos. Soc.* **1939**, *35*, 416–418. [[CrossRef](#)]
16. Le, P.Q.; Dong, F.; Hirota, K. A flexible representation of quantum images for polynomial preparation, image compression and processing operations. *Quant. Inf. Process* **2011**, *10*, 63–84. [[CrossRef](#)]
17. Zhang, Y.; Lu, K.; Gao, Y.; Wang, M. NEQR: A novel enhanced quantum representation of digital images. *Quant. Inf. Process* **2013**, *12*, 2833–2860. [[CrossRef](#)]
18. Venegas-Andraca, S.-E.; Bose, S. Storing processing and retrieving an image using quantum mechanics. *SPIE Conf. Quant. Inf. Comput.* **2003**, *5106*, 137–147.
19. Latorre, J.I. *Image Compression and Entanglement*; Tech. Rep. quant-ph/0510031; University of Barcelona: Barcelona, Spain, 2005.
20. Venegas-Andraca, S.E.; Ball, J.L. Processing images in entangled quantum system. *Quant. Inf. Process* **2010**, *9*, 1–11. [[CrossRef](#)]
21. Sun, B.; Iliyasu, A.M.; Le, P.; Dong, F.; Hirota, K. A multichannel representation for images on quantum computers using the RGB color space. In *Proceedings of the IEEE 7th International Symposium on Intelligent, Signal Processing*, Malta, Floriana, 19–21 September 2011; pp. 160–165.
22. Jiang, N.; Wang, L. Quantum image scaling using nearest neighbor interpolation. *Quant. Inf. Process* **2015**, *14*, 1559–1571. [[CrossRef](#)]
23. Jiang, N.; Wang, J.; Mu, Y. Quantum image scaling up based on nearest-neighbor interpolation with integer scaling ratio. *Quant. Inf. Process* **2015**, *14*, 4001–4026. [[CrossRef](#)]

24. Zhang, Y.; Lu, K.; Gao, Y.; Xu, K. A novel quantum representation for log-polar images. *Quant. Inf. Process* **2013**, *12*, 3103–3126. [[CrossRef](#)]
25. Li, H.S.; Zhu, Q.; Zhou, R.G.; Li, M.C.; Song, L.; Ian, H. Multidimensional color image storage, retrieval, and compression based on quantum amplitudes and phases. *Inf. Sci.* **2014**, *273*, 212–232. [[CrossRef](#)]
26. Li, P.; Xiao, H.; Li, B. Quantum representation and watermark strategy for color images based on the controlled rotation of qubits. *Quant. Inf. Process* **2016**, *15*, 4415–4440. [[CrossRef](#)]
27. Sang, J.; Wang, S.; Li, Q. A novel quantum representation of color digital images. *Quant. Inf. Process* **2017**, *16*, 42. [[CrossRef](#)]
28. Liu, K.; Zhang, Y.; Lu, K.; Wang, X.; Wang, X. An optimized quantum representation for color digital images. *Quant. Inf. Process* **2018**, *57*, 2938–2948. [[CrossRef](#)]
29. Abdolmaleky, M.; Naseri, M.; Batle, J.; Farouk, A.; Gong, L.H. Red-green-blue multi-channel quantum representation of digital images. *Opt. Int. J. Light. Electron. Opt.* **2017**, *128*, 121–132. [[CrossRef](#)]
30. Jiang, N.; Hu, H.; Dang, Y.; Zhang, W. Quantum point cloud and its compression. *Int. J. Theor. Phys.* **2017**, *56*, 3147–3163. [[CrossRef](#)]
31. Li, H.-S.; Chen, X.; Xia, H.-Y.; Liang, Y.; Zhou, Z. A quantum image representation based on bitplanes. *IEEE Access* **2018**, *6*, 62396–62404. [[CrossRef](#)]
32. Wang, L.; Ran, Q.; Ma, J.; Yu, S.; Tan, L. QRCI: A new quantum representation model of color digital images. *Opt. Commun.* **2019**, *438*, 147–158. [[CrossRef](#)]
33. Li, P.; Liu, X. Color image representation model and its application based on an improved frqi. *Int. J. Quant. Inf.* **2018**, *16*, 1850005. [[CrossRef](#)]
34. Khan, R.A. An improved flexible representation of quantum images. *Quant. Inf. Process.* **2019**, *18*, 1–9. [[CrossRef](#)]
35. Grigoryan, A.M.; Agaian, S.S. New look on quantum representation of images: Fourier transform representation. *Quant. Inf. Process.* **2020**, *19*, 148. [[CrossRef](#)]
36. Wang, L.; Ran, Q.; Ma, J. Double quantum color images encryption scheme based on DQRCI. *Multimed. Tools Appl.* **2020**, *79*, 6661–6687. [[CrossRef](#)]
37. Chao-Yang, P.; Zheng-Wei, Z.; Guang-Can, G. A hybrid quantum encoding algorithm of vector quantization for image compression. *Chin. Phys.* **2006**, *15*, 3039–3043. [[CrossRef](#)]
38. Chao-Yang, P.; Zheng-Wei, Z.; Guang-Can, G. Quantum Discrete Cosine Transform for Image Compression. *arXiv* **2006**, arXiv:quant-ph/0601043v2. [[CrossRef](#)]
39. Nodehi, A.; Tayarani, M.; Mahmoudi, F. A novel functional sized population quantum evolutionary algorithm for fractal image compression. In Proceedings of the 2009 14th International CSI Computer Conference, Tehran, Iran, 1–2 July 2009; pp. 564–569. [[CrossRef](#)]
40. Qi, F.; Zhou, H. Research of Image Compression Based on Quantum BP Network. *Indones. J. Electr. Eng. Comput. Sci.* **2014**, *12*, 197–205.
41. Du, S.; Yan, Y.; Ma, Y. Quantum-Accelerated Fractal Image Compression: An Interdisciplinary Approach. *IEEE Signal Process. Lett.* **2015**, *22*, 499–503. [[CrossRef](#)]
42. Jiang, N.; Lu, X.; Hu, H.; Dang, Y.; Cai, Y. A Novel Quantum Image Compression Method Based on JPEG. *Int. J. Theor. Phys.* **2018**, *57*, 611–636. [[CrossRef](#)]
43. Pang, C.Y.; Zhou, R.G.; Hu, B.Q.; Hu, W.; El-Rafei, A. Signal and image compression using quantum discrete cosine transform. *Inform. Sci.* **2019**, *473*, 121–141. [[CrossRef](#)]
44. Dai, J.Y.; Ma, Y.; Zhou, N.R. Quantum multi-image compression-encryption scheme based on quantum discrete cosine transform and 4D hyper-chaotic Henon map. *Quantum Inf. Process* **2021**, *20*, 246. [[CrossRef](#)]
45. Ma, Y.; Zhou, N.R. Quantum color image compression and encryption algorithm based on Fibonacci transform. *Quantum Inf. Process* **2023**, *22*, 39. [[CrossRef](#)]
46. Wang, H.; Tan, J.; Huang, Y.; Zheng, W. Quantum image compression with autoencoders based on parameterized quantum circuits. *Quantum Inf. Process* **2024**, *23*, 41. [[CrossRef](#)]
47. Ji, X.; Liu, Q.; Huang, S.; Chen, A.; Wu, S. Image Compression and Reconstruction Based on Quantum Network. *arXiv* **2024**, arXiv:2404.11994.
48. Haque, E.; Paul, M. BLOCK-WISE COMPRESSION OF THE QUANTUM GRAY-SCALE IMAGE USING LOSSY PREPARATION APPROACH. 2024. Available online: https://www.researchgate.net/profile/Md-Ershadul-Haque-3/publication/379894430_BLOCK-WISE_COMPRESSION_OF_THE_QUANTUM_GRAY-SCALE_IMAGE_USING_LOSSY_PREPARATION_APPROACH/links/66206bf243f8df018d163d27/BLOCK-WISE-COMPRESSION-OF-THE-QUANTUM-GRAY-SCALE-IMAGE-USING-LOSSY-PREPARATION-APPROACH.pdf (accessed on 12 July 2024).
49. Li, H.-S.; Qingxin, Z.; Lan, S.; Shen, C.-Y.; Zhou, R.; Mo, J. Image storage, retrieval, compression and segmentation in a quantum system. *Quantum Inf. Process* **2013**, *12*, 2269–2290. [[CrossRef](#)]
50. Brayton, R.K.; Sangiovanni-Vincentelli, A.; McMullen, C.; Hachtel, G. *Log Minimization Algorithms VLSI Synth*; Kluwer Academic Publishers: Dordrecht, The Netherlands, 1984.
51. Amankwah, M.G.; Camps, D.; Bethel, E.W.; Van Beeumen, R.; Perciano, T. Quantum pixel representations and compression for N-dimensional images. *Sci. Rep.* **2022**, *12*, 7712. [[CrossRef](#)] [[PubMed](#)]

-
52. Haque, M.E.; Paul, M.; Ulhaq, A.; Debnath, T. Advanced quantum image representation and compression using a DCT-EFRQI approach. *Sci. Rep.* **2023**, *13*, 4129. [[CrossRef](#)] [[PubMed](#)] [[PubMed Central](#)]
 53. Mastriani, M. Quantum image processing: The pros and cons of the techniques for the internal representation of the image. A reply to: A comment on “Quantum image processing?”. *Quantum Inf. Process.* **2020**, *19*, 156. [[CrossRef](#)]

Disclaimer/Publisher’s Note: The statements, opinions and data contained in all publications are solely those of the individual author(s) and contributor(s) and not of MDPI and/or the editor(s). MDPI and/or the editor(s) disclaim responsibility for any injury to people or property resulting from any ideas, methods, instructions or products referred to in the content.